

Architectural bone parameters and the relationship to titanium lattice design for powder bed fusion additive manufacturing

Martine McGregor^a, Sagar Patel^a, Stewart McLachlin^a, Mihaela Vlasea^{a,*}

^a*University of Waterloo, Department of Mechanical and Mechatronics Engineering, Waterloo, ON N2L 3G1, Canada*

Abstract

Additive manufacturing (AM) of titanium (Ti) and Ti-6Al-4V lattices has been proposed for bone implants and augmentation devices. Ti and Ti-6Al-4V have favourable biocompatibility, corrosion resistance and fatigue strength for bone applications; yet, the optimal parameters for Ti-6Al-4V lattice designs corresponding to the natural micro- and meso-scale architecture of human trabecular and cortical bone are not well understood. A comprehensive review was completed to compare the natural lattice architecture properties in human bone to Ti and Ti-6Al-4V lattice structures for bone replacement and repair. Ti and Ti-6Al-4V lattice porosity has varied from 15% to 97% with most studies reporting a porosity between 50-70%. Cortical bone is roughly 5-15% porous and lattices with 50-70% porosity are able to achieve comparable stiffness, compressive strength, and yield strength. Trabecular bone has a reported porosity range from 70-90%, with trabecular thickness varying from 120-200 μm . Existing powder bed fusion technologies have produced strut and wall thicknesses ranging from 200-1669 μm using powder bed fusion. This suggests limited overlap between current AM of Ti and Ti-6Al-4V lattice structures and trabecular bone architecture, indicating that replicating natural trabecular bone parameters with latticing is prohibitively challenging. This review contributes to the body of knowledge by identifying the correspondence of Ti and Ti-6Al-4V lattices to the natural parameters of bone microarchitectures, and provides further guidance of the design and AM recommendations towards addressing recognized performance gaps with powder bed fusion technologies.

Keywords: Additive manufacturing, Ti-6Al-4V and Titanium, Powder bed fusion, Bone micro-architecture, Orthopaedic design and bone replacement

1. Introduction

The use of Ti-6Al-4V is well established in the medical device industry [1]. Titanium and titanium alloys are ideal for replacing hard tissues, such as bone, due to their biocompatibility and excellent strength-to-weight ratio [2, 3]. Ti-6Al-4V also exhibits excellent fatigue strength and corrosion resistance

*
Email address: mihaela.vlasea@uwaterloo.ca (Mihaela Vlasea)

allowing implants to withstand the cyclic loading in high ion environments present in vivo during activities of daily living [4]. These properties of titanium and Ti-6Al-4V have led such alloys to become some of the most widely used metal materials for bone replacement and fixation procedures in the orthopaedic industry.

Despite their widespread use in the medical device industry for the replacement and repair of bone, pure titanium and Ti-6Al-4V do not have material properties similar to those of bone. Ti-6Al-4V is roughly twice as stiff as human cortical bone with up to seven times the compressive strength [5, 6, 7]. Bone is mechanoresponsive and requires regular loading in order to proliferate new bone. Implanting a stiffer material like titanium adjacent to bone can cause stress shielding of bone, resorption of the surrounding bone tissue which can lead to implant loosening and failure [8]. Therefore, it is imperative that designs of titanium and titanium alloy implants are tailored to more closely match the natural mechanical response of bone tissue. One approach to reducing stress shielding near the bone-implant interface is by light-weighting implants through latticing in an effort to reduce mechanical properties from those of the bulk modulus of the material. Additive manufacturing allows for unique design approaches thereby allowing for control of mechanical properties, while minimizing weight through unique geometries and graded material properties. Additive manufacturing technologies are of particular use in the medical device industry where implants are made for specific applications in which weight and mechanical properties are integral to implant function. Production of Ti-6Al-4V lattice structures through additive manufacturing for biomedical applications was thoroughly reviewed by Tan et al. in 2017. They concluded that optimal guidelines for lattice design in biological environments has not yet been established and that the field is rapidly and continually evolving [9]. Since the review by Tan et al. in 2017 was completed, many additional studies have successfully progressed toward this goal by manipulating lattice parameters such as porosity, pore size, and strut thickness in order to produce unit cells that more closely exhibit stiffness, compressive strength and fatigue strength of human bone. Lattice parameters widely vary across the literature and while general recommendations have been made, there remains questions as to which lattice design produces the optimal structure for implant fixation and reduction of stress shielding through mechanical property optimization.

A consideration that is notably overlooked in developing lattice structures for bone replacement is how to best model the architectural parameters of human bone. Therefore, a comprehensive literature review is needed to examine the parameters of bone micro-architecture in correspondence with lattice design parameters used in additive manufacturing. A review of existing additive manufacturing literature was completed to determine which titanium lattice parameters have been examined for bone replacement and repair implants. Lastly, recommendations are made on how to best use this information towards the design and additive manufacturing of improved titanium and Ti-6Al-4V lattice structures for bone replacement and repair.

2. Review of human bone properties relevant to lattice design

2.1. Review of human bone function

Bone is a tough, elastic tissue that gives structural support to the human body. As a living tissue, bone adapts to its environment and loading conditions through the breakdown of existing bone by osteoclasts and the proliferation of new bone by osteoblasts. This process leads bone to exhibit mechanoresponsive behaviour, wherein the more it is loaded, the thicker and denser it becomes. Bone can be categorized into two main types: cortical bone and trabecular bone, see Figure 1. Different bones in the human body consist of different amounts and configurations of cortical and trabecular bone. Long bones, such as the femur, tibia, radius, and humerus, have a long shaft made up of primarily cortical bone. The articulating ends of long bones are made of primarily trabecular bone contained by a thin shell of cortical bone. Short bones, such as vertebrae, carpals, and tarsals, are made primarily of trabecular bone with a thin cortical shell making them strong and compact. Cortical bone density and trabecular bone density are important indicators of bone strength, and decrease with age, for instance by approximately 0.41% and 0.65% per year, respectively, for women ages 70 to 87 years old [10]. However, studies have demonstrated that trabecular bone has a higher correlation to bone strength than cortical bone [11].

2.2. Trabecular bone

Trabecular bone, or cancellous bone, is a lattice-like structure that allows bone to maintain its strength, while being relatively lightweight. Trabecular bone is primarily located at the articulating ends of long bones and in the body of short bones, which allows for improved load transfer through these structures. The exact configuration of trabecular bone micro-structure is still being discovered. The most established theory characterizes the trabeculae, or struts, by their thickness, spacing, number and spatial configuration. Measurement techniques for these parameters are well established and widely published to comparatively describe trabecular bone quality, with more and thicker trabeculae suggesting better bone health [14]. However, emerging and more advanced geometric models consider the shape of trabecular surface and the rod vs plate-like structures of trabecular architecture in greater detail [15, 16].

The integrity of trabecular bone microstructure is often used as an indicator for overall bone health. At any given age, men have a higher trabecular bone mass than women, but decreases in trabecular bone density due to aging are similar in women and men [17, 18, 19, 20, 21]. Age-related changes cause buckling of trabeculae due to a decrease in the number and thickness of trabeculae, and an increase in trabeculae length [14]. Collectively, these changes result in a decreased trabecular density; however, the pathology of this reduction differs in men and women [14]. In women, the decrease in

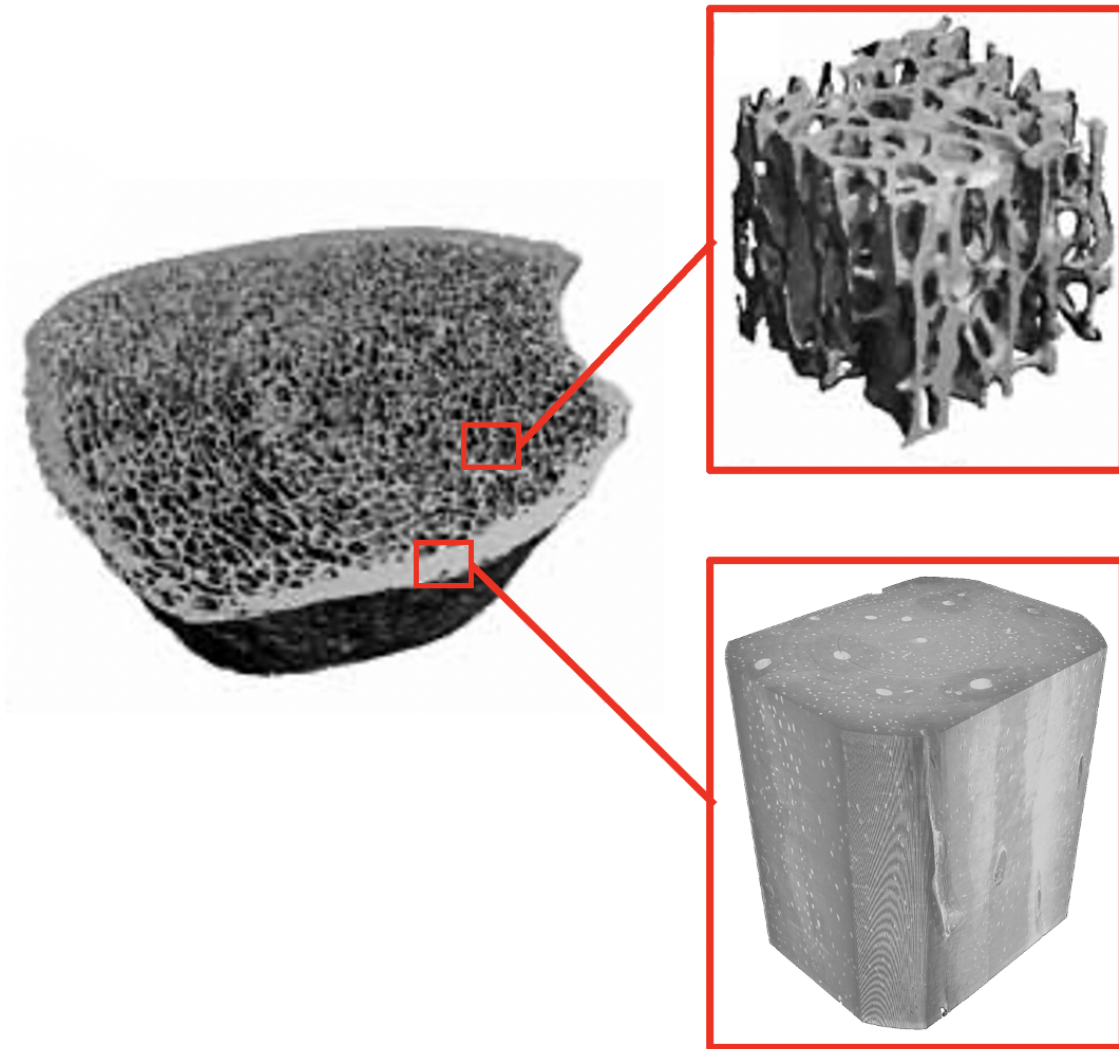


Figure 1: Human bone can be categorized into two main types: cortical and trabecular. Cortical bone is the stiffer, more dense bone which encapsulates short bones, the ends of long bones and comprises the shaft of long bones. Trabecular bone is the lattice like structure which makes up the majority of short bone structure as well as the ends of long bones.

This figure was adapted from the μ CT work of Lui et al. and Gauthier et al. [12, 13]

bone volume occurs primarily due to a decrease in the number of trabeculae, whereas in men, it may be predominantly attributed to the thinning of trabeculae [17, 22]. The decrease in trabeculae in women is related to menopause, where less estrogen is produced, which increases bone reabsorption [23]. Therefore, in making design considerations for orthopaedic medical devices, the patient population, age and sex should be carefully considered. Changes may be made to lattices designs to model the reduction in bone density with age. Lattice structures with fewer shorter features may better represent aging female bone and lengthening features may better model aging male bone. Lower density lattice designs should also be considered for older adults and post-menopausal women.

2.2.1. *Micro-architecture of trabecular bone*

The micro-structure of trabecular bone can be characterized by the individual trabeculae and the spaces between them. To determine bone porosity, the volume of bone (BV) is divided by the total volume (TV) for a given sample (BV/TV). Other groups have also compared total bone surface area (BS) with respect to bone volume (BS/BV) or total specimen volume (BS/TV) as another form of trabecular quality indicator. Trabeculae are further characterized by thickness of individual vertical trabeculae (TbTh), the distance between trabeculae (TbSp), and the number of trabeculae that intersect with a given two-dimensional distance metric (TbN), typically 1 cm, as shown in Figure 2.

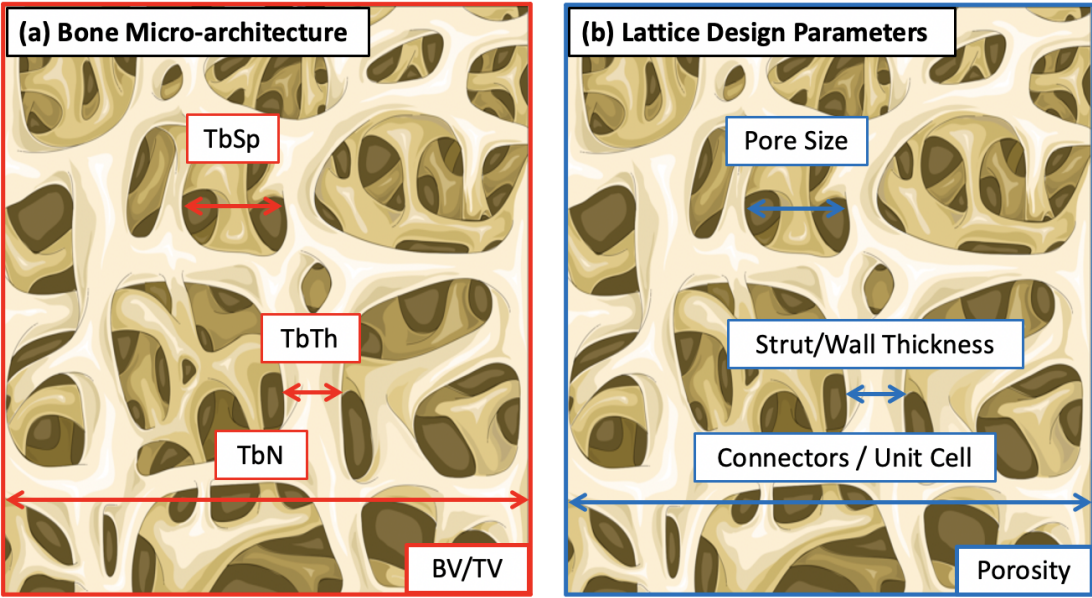


Figure 2: Commonly reported measurements of trabecular bone microstructure (red) may be used to describe lattice parameters commonly used in additive manufacturing (blue).

Methods of calculating bone architectural parameters may vary between studies; however, the technique proposed by Hildebrand et al. is the most widely accepted in general literature, as shown in

Table 1: The Hildebrand et al. method for calculation two dimensional trabecular measurements from known bone volume fractions.

Trabecular Bone Parameter	Measurement/Calculation
Apparent bone density	BV/TV
Porosity	$1 - BV/TV$
Bone surface fraction	BS/BV or BS/TV
Trabecular thickness	$TbTh = 2 BV/BSs$
Trabecular spacing	$TbSp = 2 (TV-BV)/BS$
Trabecular number	$TbN = 0.5 BS/TV$

Table 1. Hildebrand et al. proposed a two-dimensional (2D) plate model that allows for calculation of 2D parameters such as TbTh, TbSp and TbN [24].

Trabecular bone density and parameters vary greatly with anatomical location, as shown in Figure 3. When determining design considerations for bone replacing implants, anatomical location and device function should be considered. Hildebrand et al. undertook an in-depth in vitro study comparing the micro-architecture of trabecular bone at different sites across the skeleton [24].

2.2.2. Mechanical properties of trabecular bone

The mechanical properties of trabecular bone vary significantly with respect to bone density. For instance, trabecular bone density predicts 81% of axial strength variation in the human tibia [26]. The porosity of human trabecular bone ranges from 40-95%, dependent on skeletal location, bone region, and population parameters [27]. Stiffness and strength of trabecular bone is significantly greater in the direction of loading, z-axis, and lower, but similar in other directions, x- and y-axis respectively. Young's modulus of trabecular bone can range from 1-5 GPa along the axis of loading and 50-700 MPa off-axis. As such, the compressive and tensile strength of trabecular bone ranges from 0.1-30 MPa and 6-8 MPa, respectively [28, 29, 30].

2.3. Cortical bone

Cortical bone, or compact bone, is much more dense than trabecular bone and acts as a stiff outer layer for short bones, joints in long bones and the sole composition of the hollow shafts of long bones. Cortical shells allow for a continuous surface at the joints for ligamentous and tendonous attachment. Cortical bone improves the overall fracture toughness and provides structural integrity to limbs allowing for gross movement.

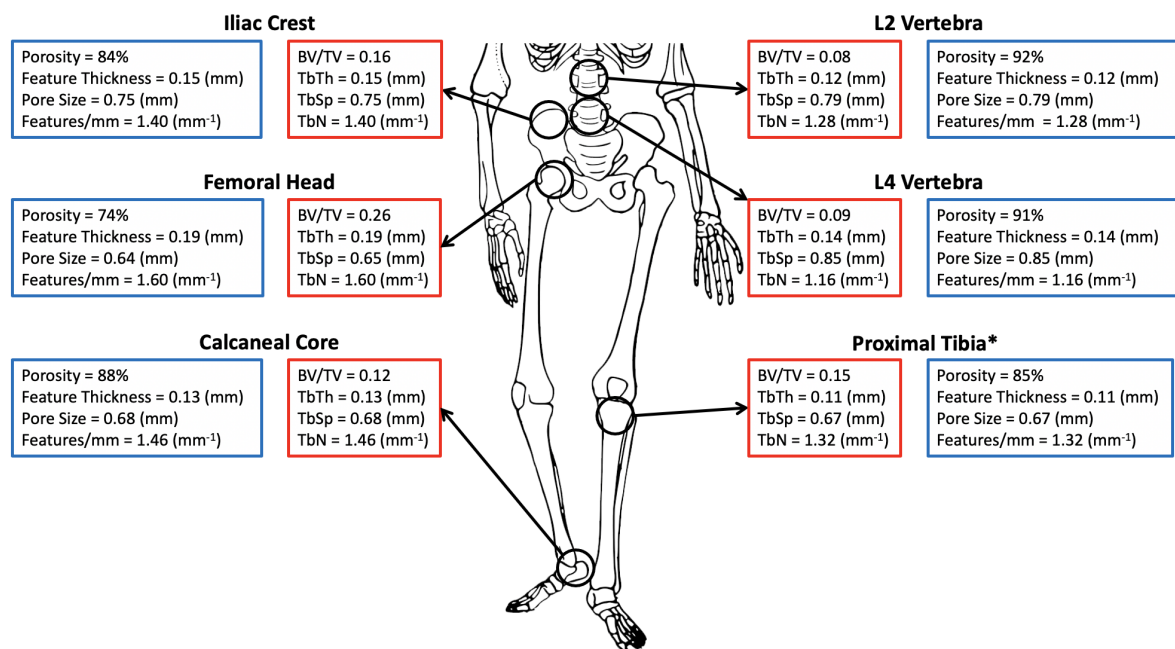


Figure 3: A comprehensive summary of two- and three-dimensional measurements of trabecular bone at the femoral head, iliac crest, calcaneal core, L2 vertebra and L4 vertebra as described by Hildebrand et al. [24]. The mean data reported by Hildebrand et al. was supplemented with Thomsen et al.'s report of trabecular bone parameters at the proximal tibia to form an original visual representation was generated to more clearly communicated this information [25]*. Bone microstructure data is outlined in red and suggested translation to lattice design parameters is outlined in blue. The values listed represent the mean value of the each measurement.

2.3.1. Micro-architecture of cortical bone

Cortical bone is much more dense than trabecular and exhibits only 5-15% porosity [27]. It is well documented that cortical bone porosity and thickness decrease with age [17]. Interestingly, microstructural analysis has shown that the cortical bone stiffness, fatigue strength and fracture toughness decrease with age [31]. It should also be noted that studies have indicated that the decrease in cortical bone density is significant in women, but insignificant in men [17].

2.3.2. Mechanical properties of cortical bone

Cortical bone is widely considered to be transversely isotropic, with mechanical properties along the axis of loading, or the z-axis, being significantly greater than those in the x- and y- axis. The transversely isotropic mechanical properties of human cortical bone have been collated from literature to provide a holistic visual representation, see Figure 4 [28, 29, 32].

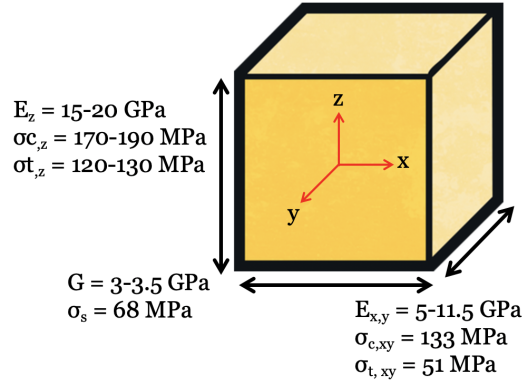


Figure 4: Cortical bone exhibits transversely isotropic mechanical properties with nearly double the stiffness occurring along the axis of loading. [28, 29, 32] Young's modulus, ultimate compressile strength, and ultimate tensile strength in the longitudinal direction are denoted E_z , $\sigma_{c,z}$, and $\sigma_{t,z}$ respectively. The subscript "x,y" is given to denote mechanical properties in the transverse axes.

3. Additively manufactured lattices for bone replacement

Computer aided design (CAD) and additive manufacturing (AM) have advanced in technological readiness, enabling the regulatory pathways and component mechanical performance to be ready for wide-scale application in the medical device industry [33, 34]. Existing literature on additively manufactured medical devices for bone replacement or augmentation is widely spread based on target audience, research background, and study type. Research of additively manufactured medical devices can be found in surgical, tissue, biomedical engineering, additive manufacturing and/or material science journals. Collating the existing body of research into a cohesive overview proves challenging, as the focus of research covers a wide array of topics from AM process parameters, material properties, and biocompatibility, all the way to medical function and clinical outcomes. In order to review metal additive manufacturing as a technology for bone replacement an overview of metal AM and lattice design approaches has been included below.

3.1. Review of additive manufacturing for metals: powder bed fusion

Laser powder bed fusion (LPBF) and electron beam powder bed fusion (EB-PBF) are AM processes in which a heat source is directed towards a powdered material to micro-weld the material together, layer-by-layer. During the LPBF process, a fine laser beam (with beam spot sizes (σ) generally between 50 to 100 μm) is generally directed through a series of lenses towards an X-Y plane via scanning mirrors which direct the beam towards the build platform. In EB-PBF (beam spot sizes (σ) generally greater than 200 μm) the same phenomenon is achieved through a directed high energy electron beam rather than a laser. In both cases, the build platform contains a bed of powdered material. As each layer

is micro-welded together, the build platform lowers and a new layer of powder is deposited over the build platform with a blade or rake. This process is repeated layer-by-layer until the part is complete. Post-processing may be required to ensure certain material properties, part geometry and/or surface finish.

Some of the major advantages of LPBF when compared to other metal AM processes are its fine resolution [35], wide range of materials available for the technology [36], and the potential to obtain performance superior to conventional manufacturing processes [37]. The superior resolution of LPBF when compared to direct energy deposition (DED) and EB-PBF makes it an ideal candidate for manufacturing intricate lattices used in light-weighting parts, as well as for manufacturing complex lattice structures with fine feature sizes. LPBF also has the largest range of metal material options of any metal AM technologies. One such material is Ti-6Al-4V, a widely used biomaterial in the medical device industry. There are some benefits to considering EB-PBF for the fabrication of biomedical devices: the reduction in residual stresses resulting in reduced part distortion due to the elevated environment temperature during production, the powder layer is pre-heated into a powder cake which serves as a thermal dissipation pathway, reducing the need for extensive support structures except for part substrate anchoring requirements. As such, both LPBF and EB-PBF will be considered in this work, with a focus on lattice structure design, performance, and manufacturability for orthopaedic bone replacement and augmentation devices.

3.2. Review of lattice designs

Lattice structures are a form of hierarchical design structures used to minimize unnecessary material with respect to design function. Lattices are typically designed for a specific application or function such as reducing weight while maintaining mechanical strength, or improving energy absorption characteristics of a design component [38, 39]. Lattice structures can be categorized into two main structure types: designed cellular lattices and stochastic (random) lattices [40].

3.2.1. Designed cellular structures

The majority of lattice structures can be categorized as cellular structures that are made up of unit cells with distinct, repeatable features. Cellular lattice structures are made up of struts and/or walls that are repeatedly interconnected in 3D-space by nodes. Designed cellular lattices can then be further categorized into periodic and pseudo-periodic lattices that are of homogeneous or heterogeneous organizations [41]. The periodicity of a lattice refers to the size of the unit-cells throughout the structure and homogeneity refers to the thickness of the unit-cell elements such as struts and walls. Therefore, a periodic lattice would have a uniform unit-cell size throughout its structure and a pseudo-periodic structure would have variable unit cell size. Both periodic and pseudo-periodic lattices can be further

categorized into homogeneous or heterogeneous wherein they have either uniform or gradient-based strut and/or wall thickness, respectively [41].

3.2.2. Stochastic lattices

Stochastic, or random, lattice structures consist of irregular and non-periodic cells resulting in a network of interconnected struts and/or surfaces. Unlike other lattice structures there is no distinct cellular features that are repeated in 3D space and each cell contains a unique configuration of struts and nodes. Stochastic lattices have superior performance under both compressive and shear loading when compared to regular lattice structures [42]. However, due to their complex design, there are not as many readily available tools for the design and implementation and therefore they are not as commonly examined in literature. The final lattice type to be examined are spinodoid lattices [43], which are a subset of stochastic lattices and surface lattices. The major differentiating characteristic of spinodal lattices is that they are non-periodic. This allows for a larger design space and more achievable control of the directional mechanical properties. The benefit of spinodal surfaces is that they are immune to the symmetry-breaking defects present in cellular lattices, thus improving their mechanical properties [43].

3.2.3. Strut- vs surface-based lattices

Another form of categorization for lattice structures is by the cellular organization of structure. The two cellular organizations of lattice structures are strut-based lattices and surface-based lattices. Strut-based lattices are generated by determining unit cell size, the number nodes located throughout the unit cell, and the number and configuration of connectors linking each node to each other. Porosity of the lattice may be controlled directly, or strut thickness may be selected as the control variable for lattice density. Surface-based lattices consist of a locus of points defined by a function. The most commonly used and discussed surface lattice family are triply period minimal surface (TPMS) lattices. TPMS lattices are defined by implicit functions for which the function has a constant value. TPMS structures may be periodic or pseudo-periodic and heterogenous or homogeneous.

4. Review methodology

A comprehensive literature review was completed to better understand how lattice parameters are controlled in additively manufactured titanium and titanium alloy parts aimed at replacing or augmenting bone. In order to collect the most relevant data, all powder bed additive manufacturing processes were considered, pure titanium and titanium alloys were considered, and all study types were considered; however, studies were only included when bone was the target tissue for replacement, repair and/or augmentation, to enhance the relevant scope of the designed architectures. A total of 50 journal

articles fit the above criteria and the effect of lattice design parameters on mechanical properties was extracted and examined [44, 45, 46, 47, 48, 49, 50, 51, 52, 53, 54, 55, 56, 57, 58, 59, 60, 61, 62, 63, 64, 65, 66, 67, 3, 68, 69, 70, 71, 72, 73, 74, 75, 76, 77, 78, 79, 80, 81, 82, 83, 84, 85, 86, 87, 7, 88].

Existing literature describing additive manufactured titanium implants for bone replacement fits into two main categories of critical design focus: studies focused on improving osseointegration and studies focused on targeted mechanical properties. Osseointegration refers to bone's ability to grow on the surface of the implants and infiltrate the porous implant to improve implant fixation. In general, literature focused on osseointegration was found to have fewer reported AM and lattice parameters provided and often focused on *in vivo* results in animals or human case studies. The primary target audience for this category seems to be medical and academic researchers interested in bone tissue mechanics, growth and healing and secondarily, the additive manufacturing community. The other category of literature aims at matching the mechanical properties of bone by controlling the lattice design parameters and by controlling the printing process parameters of the respective technologies. Literature focused on matching mechanical properties of lattice structures to bone, primarily targets the additive manufacturing community with implications for bone tissue and device design being secondary suggestions. It is noteworthy to highlight this lack of apparent synergy between the two categories; such synergy is required to ensure advancements in this field.

A wide cross-section of lattice design information was collected from the bone and AM focused journals and was collated in the associated Data in Brief. Key parameters collected include: Young's modulus, compressive strength, lattice porosity, pore size, feature thickness, lattice type and material used. When studies compared more than one lattice design parameter, all relevant data points were collected in order to make the most robust comparison possible. Data points were then plotted on alongside Ashby plots for trabecular and cortical bone to assist in making recommendations for future lattice designs focused on titanium implant designs for bone repair and replacement (CES EduPack software, Granta Design Limited, Cambridge, UK, 2009).

5. Results and discussion

5.1. Lattice considerations

5.1.1. Porosity

The exercise of understanding trabecular and cortical bone porosity provides insight into the porosity required to match the structural properties of bone through titanium and Ti-6Al-4V latticing [48, 49, 53, 55, 56, 57, 58, 61, 89, 62, 63, 64, 87, 90, 68, 70, 71, 73, 74, 77, 78, 80, 81, 82, 88, 83, 84]. The most common lattice parameter reported in literature focused on additively manufactured titanium and titanium-alloy lattice structures was macro-scale porosity or void fraction. Designed lattice porosity

varied from 15% to 97% with the majority of studies reporting a designed porosity between 50-70%. Titanium and titanium alloy lattices within this designed porosity range were successful in matching the stiffness of cortical bone which is known to be 5-15% porous. However, few were successful in matching mechanical properties of trabecular bone, as depicted in Figure 5. Trabecular bone is 70-90% porous, and through this review, it was determined that titanium and Ti-6Al-4V lattices must have a designed porosity of >80% to replicate mechanical properties of trabecular bone. These findings indicate that matching material properties of titanium and Ti-6Al-4V via latticing may be challenging with existing AM technologies.

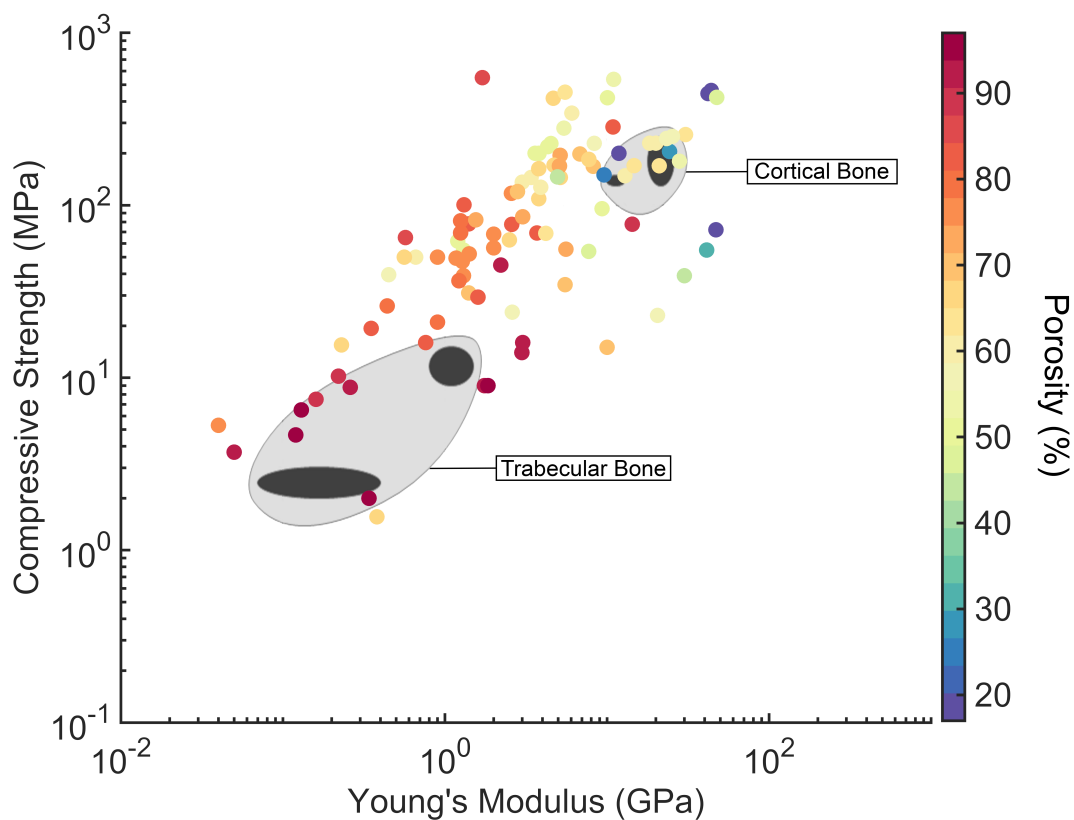


Figure 5: Porosity is the most common lattice parameter reported in literature. Compressive strength and Young's modulus of additively manufactured lattice structures were plotted over the Ashby plots of human trabecular and cortical bone. Lattice porosity ranged from 15-97% and was plotted in a gradient to depict how best to design for material property matching [48, 49, 53, 55, 56, 57, 58, 61, 89, 62, 63, 64, 87, 90, 68, 70, 71, 73, 74, 77, 78, 80, 81, 82, 88, 83, 84].

5.1.2. Pore size

Two-dimensional micro-architecture measurements of bone can also be described in terms of lattice parameters. When considering TbSp as a surrogate bone pore size, Hildebrand et al. reported a

range from 638 μm in the femoral head to 854 μm in the lumbar spine [24]. In the literature focused on osseointegration for additively manufactured titanium lattice designs, the lattice parameter most commonly reported was pore size. The pore sizes reported ranged from 100-1500 μm . Recommendations for tailoring pore size to optimize bone in-growth or osseointegration were consistent and conclusions were drawn surrounding an acceptable range for optimal boney ingrowth. A minimum pore size of 200 μm should be considered to allow for initial cell adhesion [55]. However, to maximize cell proliferation and limit cell occlusion, large pore sizes >1000 μm are recommended [89]. Therefore, a functionally graded lattice which combines small pores for initial cell attachment and large pores to avoid cell occlusion would account for both recommendations [59, 91]. Pore size did not exhibit a trend with respect to compressive strength and Young's modulus as seen in Figure 6 [48, 49, 53, 55, 57, 58, 61, 89, 63, 64, 90, 68, 73, 92, 77, 80, 82, 88]. Therefore, pore size should be viewed as a design parameter for biological reaction rather than mechanical function.

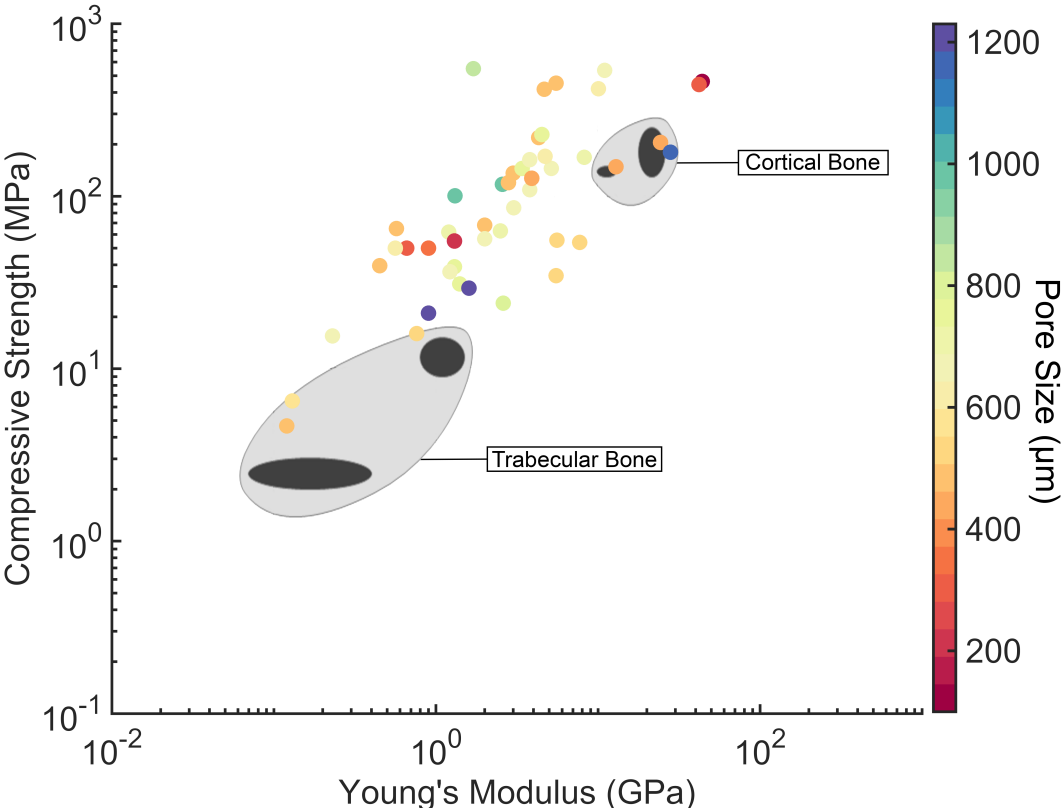


Figure 6: Designed pore size of additively manufactured Ti and Ti-6Al-4V lattice structures was plotted in a gradient over a compressive strength versus Young's modulus Ashby plot for human trabecular and cortical bone tissues to depict how best to design for material property matching [48, 49, 53, 55, 57, 58, 61, 89, 63, 64, 90, 68, 73, 92, 77, 80, 82, 88].

5.1.3. Feature Thickness

Trabecular thickness can be related to feature, strut or wall thickness. Across the human skeleton, trabecular thickness varies from roughly 120-200 μm [24]. This is lower than 400 μm , or the minimum feature thicknesses typically recommended for powder bed fusion. This is most likely due to the part resolution that can be obtained through current additive manufacturing technologies. While there were no strong trends in the effect of feature thickness on compressive strength and Young's modulus for the feature size range captured in these studies, decreasing feature thickness is one way to control lattice porosity, which is critical to manipulating mechanical properties, as seen in Figure 7 [48, 49, 56, 57, 58, 61, 62, 63, 64, 87, 70, 74, 77, 78, 83, 84].

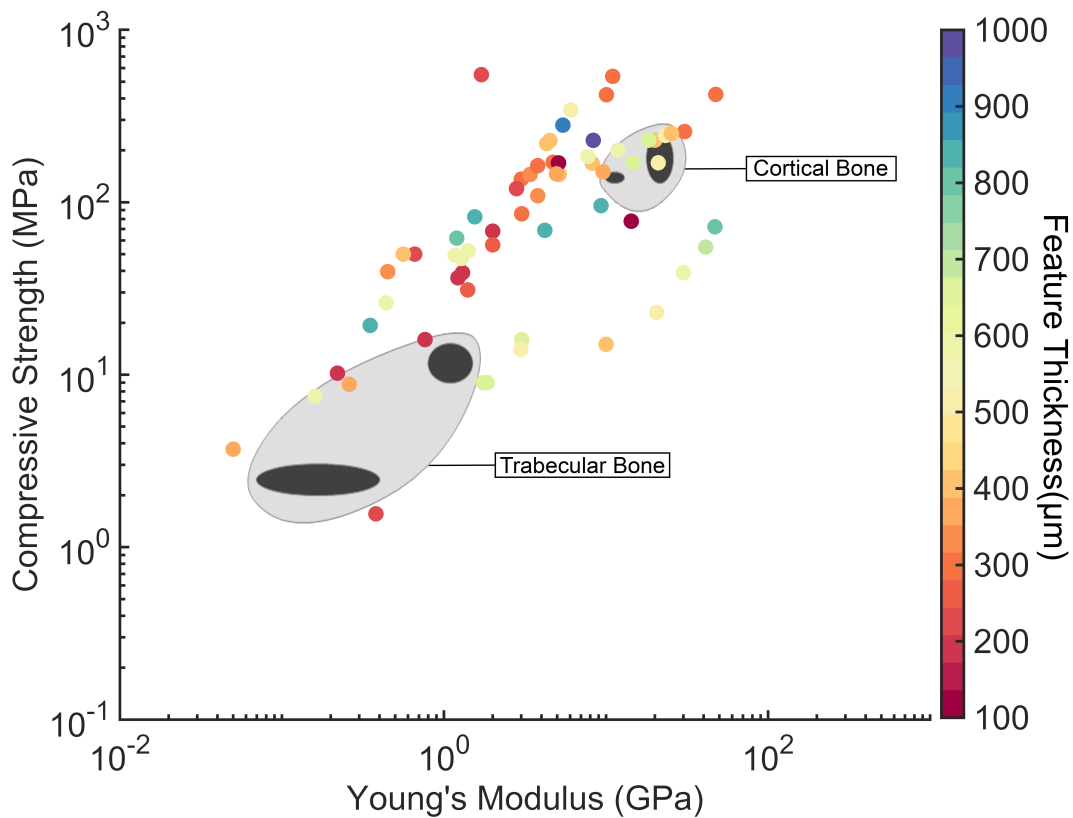


Figure 7: Feature thickness was plotted in a gradient over a compressive strength versus Young's modulus Ashby plot for human trabecular and cortical bone tissues to depict how best to design for material property matching [48, 49, 56, 57, 58, 61, 62, 63, 64, 87, 70, 74, 77, 78, 83, 84].

5.1.4. Lattice type

When compared to strut-based lattices, surface-based lattices, such as TPMS structures, allow for better osseointegration [91]. This is thought to be due to the increased surface area available in

surface-based lattices for cellular adhesion. However, the designed lattice porosity needed to match the mechanical properties of trabecular bone requires very thin wall thickness. Surface lattices also have lower stress concentrations under angular load simulation, which may make them further suitable for bone implants [91]. A recent study from Alabort et al. showed promising results for reaching the mechanical properties of trabecular bone through the use of TPMS surface lattices, specifically Schwartz’s diamond surface structures [73]. In this review, lattice type had no noticeable influence on compressive strength nor Young’s modulus of titanium and Ti-6Al-4V lattice structures aimed at human bone replacement, see Figure 8 [48, 49, 56, 61, 89, 62, 63, 64, 68, 70, 73, 74, 77, 78, 80, 93, 82, 88, 83].

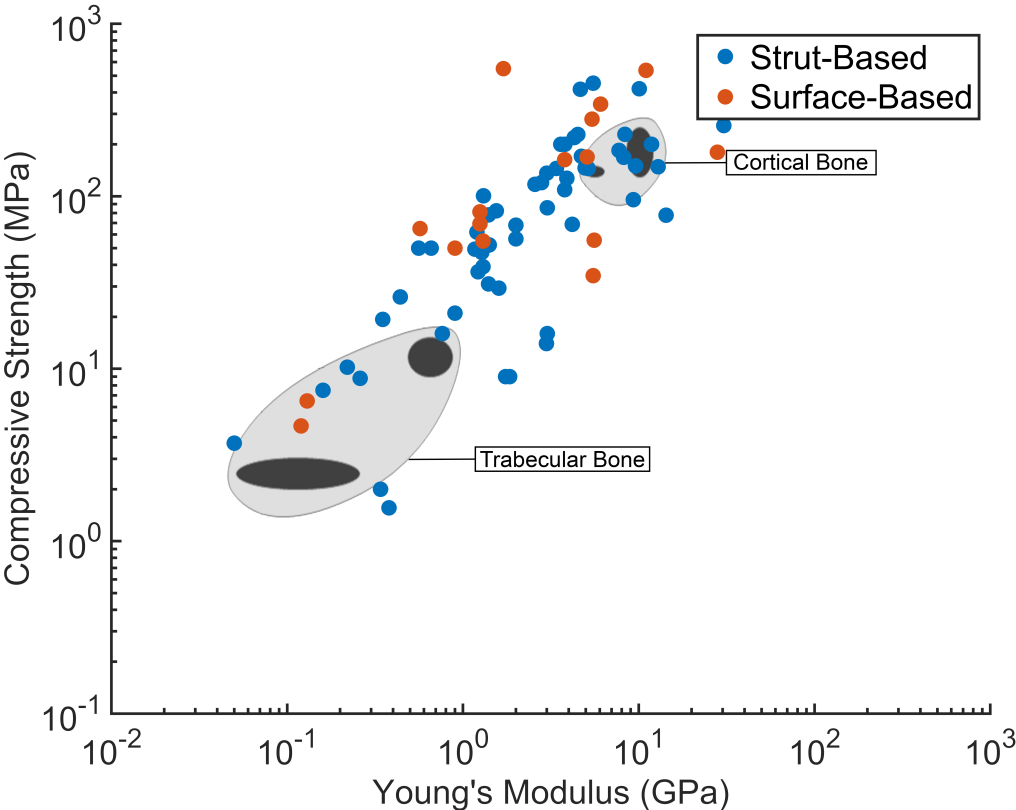


Figure 8: Lattice type, strut- vs surface-based, was plotted in a gradient over a compressive strength versus Young’s modulus Ashby plot for human trabecular and cortical bone tissues to depict how best to design for material property matching [48, 49, 56, 61, 89, 62, 63, 64, 68, 70, 73, 74, 77, 78, 80, 93, 82, 88, 83].

5.1.5. Material selection

Finally, material choice was examined and Ti and Ti-6Al-4V lattices were compared for their ability to achieve comparable Young’s Modulus and compressive strength to human bone tissues [48, 49, 53, 55, 57, 58, 61, 89, 62, 63, 64, 90, 68, 70, 71, 73, 74, 77, 78, 80, 81, 82, 88, 83, 84]. Despite

having slightly different bulk moduli, Ti and Ti-6Al-4V lattices did not differ in ability to reach bone properties, see Figure 9. This may be due to other lattice design decisions, such as porosity, pore size and feature thickness, that were made to tailor overall mechanical properties.

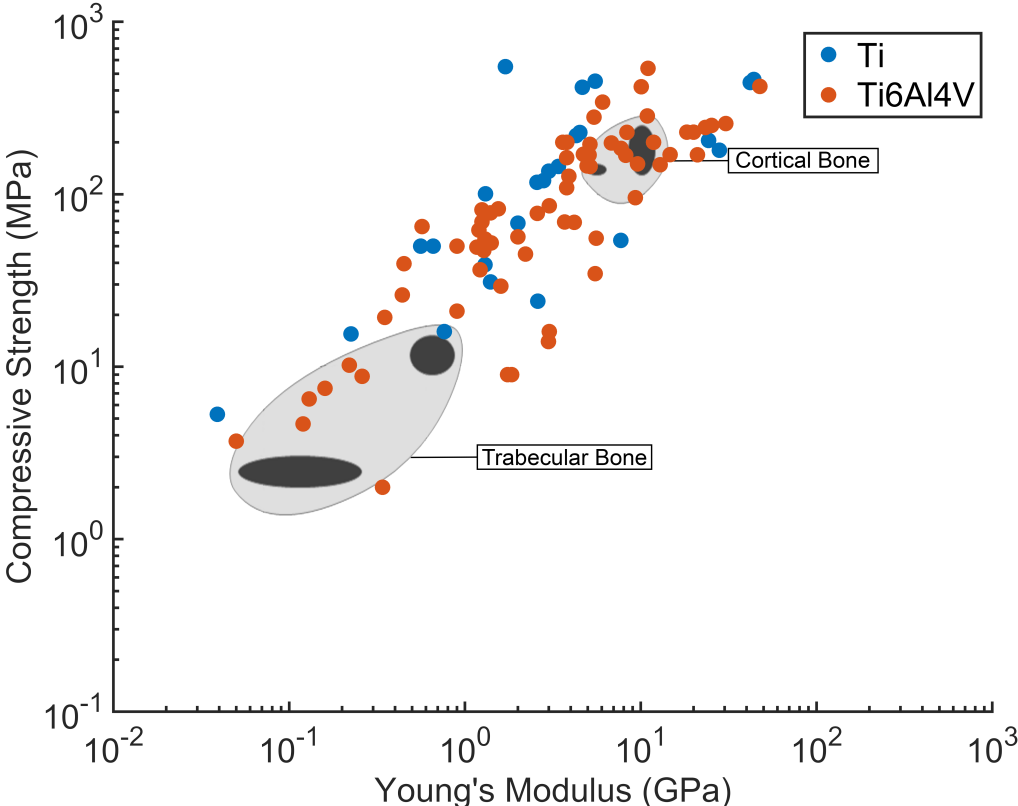


Figure 9: Material type, Ti vs Ti-6Al-4V, was plotted in a gradient over a compressive strength versus Young's modulus Ashby plot for human trabecular and cortical bone tissues to depict how best to design for material property matching [48, 49, 53, 55, 57, 58, 61, 89, 62, 63, 64, 90, 68, 70, 71, 73, 74, 77, 78, 80, 81, 82, 88, 83, 84].

5.2. Manufacturability Considerations

The potential of powder bed fusion AM technologies such as LPBF and EB-PBF to manufacture parts with higher geometric complexity compared to traditional manufacturing, makes them well suited for fabricating lattice structures mimicking bone properties. The complex features involved in the design of most lattice structures tests the manufacturability limits of LPBF and EB-PBF. This is mainly because most lattice structures used for bone replacements require fine feature sizes, particularly to replace trabecular bone. The minimum feature size strongly depends upon the beam spot size used which is generally between 50-100 μm for LPBF and $>200 \mu\text{m}$ for EB-PBF. Additionally, lattice structure designs generally incorporate numerous overhanging features within a unit cell, which are

challenging to produce by both LPBF [94, 95] and EB-PBF [96, 97, 98]. Pushing the design boundaries in LPBF and EB-PBF to achieve lattice architectures tailored for bone replacement and augmentation necessitates an understanding of the three main categories of manufacturability challenges which arise in these AM technologies - defects (micro-porosity within the manufactured lattice structure), surface roughness, and geometric fidelity.

5.2.1. Porous defects

Due to the fatigue strength and stiffness requirements associated with manufacturing titanium-based bone replacements, understanding defects is important, as they directly impact both stiffness and fatigue life of a given AM part. It is well documented in AM literature that defects are particularly deleterious for fatigue properties [99, 100, 101]. In most of the articles reviewed in this work, stiffness values and lattice design details were commonly reported for titanium alloy lattice structures used for bone replacements, but a study into the defects within the lattice structures and their effects on fatigue life were less frequently reported.

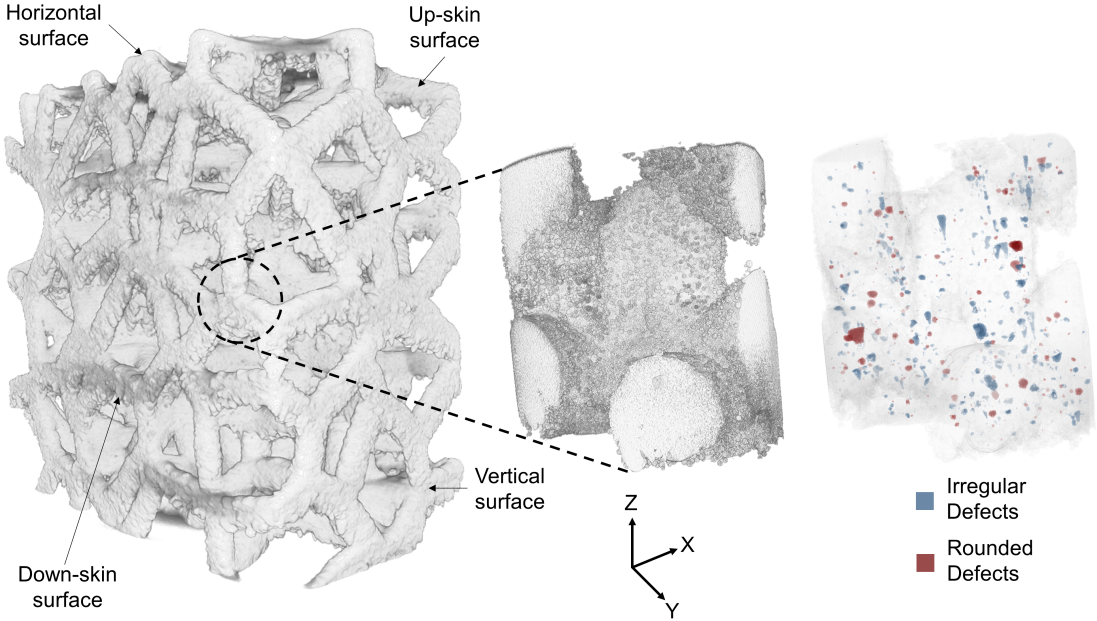


Figure 10: A three-dimensional XCT visualization of the different types of surfaces observed in a laser powder bed fusion Ti-6Al-4V Voronoi lattice structure with respect to the build orientation along the Z-axis (left), a high resolution XCT image of a portion of the Voronoi lattice structure (center), visualization of the defects inside the printed lattice structure (right).

The amount of defects and their typical morphology observed in powder bed fusion (PBF) AM depends on the process parameters used for manufacturing a given lattice structure. A low energy input is typically associated with the formation of irregularly shaped lack of fusion defects [102], with a high

aspect ratio (width/depth) which are known to be more detrimental to the fatigue strength of lattice structures [100], when compared to rounded keyhole defects typically associated with high energy inputs [102]. It is important to note that the presence of rounded or irregularly-shaped defects is not only dependent upon the energy input, but rather requires an understanding of PBF process parameters, particularly power, beam velocity, beam spot size, powder layer thickness, and hatching distance. It is quite possible to obtain irregularly shaped, lack of fusion defects within a lattice structure that uses high energy keyhole mode parameters, as shown by an X-ray computed tomography visualization of the defect space within a Ti-6Al-4V Voronoi lattice structure manufactured by LPBF in Figure 10. A summary of the LPBF processing details and XCT measurements of the lattice structure are provided in the associated Data in Brief.

5.2.2. Surface roughness

Surfaces in PBF parts are generally identified with their orientation with respect to the build plate used for manufacturing as shown by the left image in Figure 10. The four type of surfaces shown in Figure 10 include - horizontal up-facing surfaces that are parallel to the build plate (along the XY plane), vertical surfaces that are perpendicular to build plate (along the Z axis and also known as side-skin surfaces), upward facing surfaces (known as up-skin surfaces) which are typically on an incline, but facing upwards, and downward facing surfaces (known as downskin surfaces) [103]. Since most lattices used for bone replacement are comprised of a combination of all four surface types, these surfaces are distinctly different contributors towards the final surface roughness in the printed lattice structures. Side-skin (vertical) surfaces [103, 104] and down-skin surfaces [105, 106, 101] are associated with a higher number of challenges when trying to obtain lower surface roughness values in as-printed PBF lattices, when compared to horizontal up-facing and up-skin surfaces.

In PBF AM processes, an interplay between process parameters, build file characteristics, machine characteristics, and powder characteristics drive the final surface topography of a given lattice structure. More precisely, processing parameters such as power, scan speed and layer thickness, build file characteristics such as feature geometry, feature orientation, feature location on the build plate, and beam path strategy, machine and energy source characteristics such as beam spot size, laser beam quality, and gas flow (for LPBF), and powder morphology and size distribution are some of the primary drivers for roughness of a given lattice structure.

Out of the four influencing factors, PBF process parameters are known to have the greatest effect on roughness and are also the most readily controllable for a given lattice. Horizontal and up-skin surface roughness possibly depend upon the overall size of the melt pools [107, 108], where the roughness on these surface features generally includes visibility of the melt pool tracks alongside partially fused adhered powder, particularly for the up-skin surfaces. Down-skin surface features include partially

fused adhered powder as sources of coarse roughness and dross (at higher energy inputs); overall, the down-skin roughness strongly depends on the melt pool depth [106, 107]. A melt pool depth close to the powder layer thickness is generally considered to be useful for lowering down-skin surface roughness values [106]. Remelting scans of horizontal, up-skin, and down-skin surfaces are known to improve the roughness values of these surfaces [107]. Side-skin (vertical) surfaces are an exception, wherein remelting would generally not help further improve surface roughness, when compared to a well-executed first side-skin scan [109]. Side-skin surfaces are generally dominated by partially fused adhered powder in PBF, but the effects of powder can be reduced by an appropriate energy input selection which enables a dominance of melt pool track features on the side-skin that are associated with lower surface roughness values [102, 104].

Surface roughness of AM titanium lattices for bone replacement applications has been previously examined in literature. Webster and Ejiófor examined osteoblast proliferation on 90-95% dense Ti and Ti-6Al-4V structures. They reported that osteoblasts prefer titanium surfaces with nanometer topology features [110]. Conversely, Zhang et al. reported that a surface roughness of 1-2 μm improved osteogenic properties of titanium bone implants [92]. There is still no consensus on optimal surface topology and roughness for osseointegration and adhesion, as changes in the microstructure and nanostructure of lattice surfaces both influence the cell response in bone tissues [111].

5.2.3. Geometric fidelity of lattice features

The fine and complex features involved in the CAD of most lattices used for bone replacements test the manufacturability limits of both LPBF and EB-PBF. This implies that a lattice structure with a fine feature size might print successfully, but not conform to the original CAD, leading to dimensional inaccuracies. Inaccuracies in additively manufactured lattices would directly impact their performance as bone replacements, since the reality of the AM structure would differ from the modelling efforts and design decisions used to determine the feature size and morphology of the lattice. Attempts at reporting the geometric fidelity of AM lattices, however, have been scarce.

In literature where dimensional inaccuracies have been reported, significant under-sizing and over-sizing of additively manufactured lattices compared to the original CAD are observed, sometimes over 100%, as reviewed by Echeta et al [101]. Dimensional inaccuracies in AM lattices depend on numerous factors, including build file setup (location, orientation, recoater offset angle, etc.) [112], PBF process parameters [113, 103], CAD file resolution [114], powder size and morphology [35, 115], and beam properties such as wavelength, operating mode, shape and quality [116, 117].

When it comes to strut-based lattices, higher dimensional inaccuracies are reported for diagonal and horizontal struts, when compared to vertically printed struts [93, 118, 119]. This is because horizontal and diagonal struts contain the highest proportion of overhanging features which are known to have the

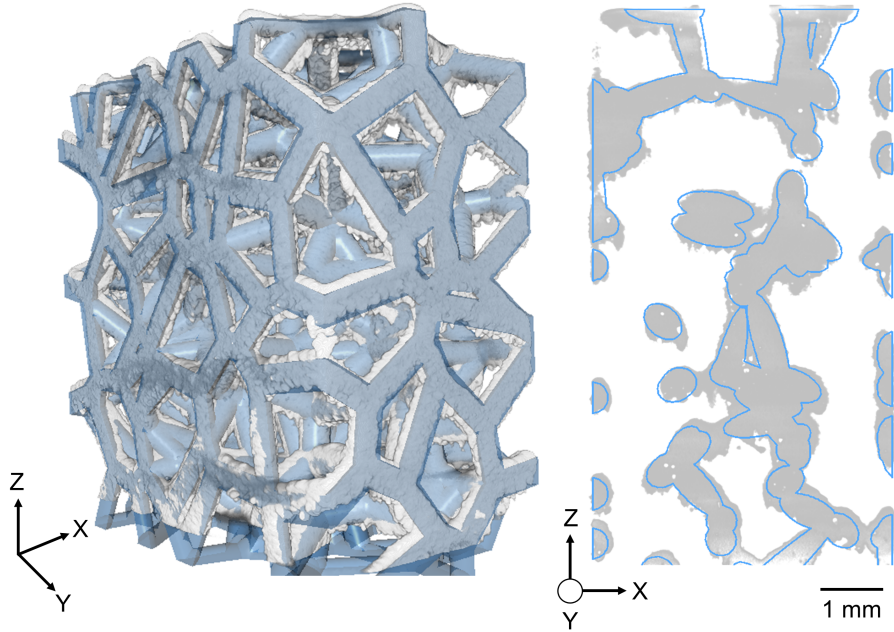


Figure 11: A 3D comparison of the XCT visual (shown in grey) and the original CAD (shown in blue) of a Ti-6Al-4V Voronoi lattice structure manufactured by laser powder bed fusion (left) and a 2D comparison of a slice along the XZ plane of the XCT visual (shown in grey) and the original CAD (shown in blue) of the lattice structure (right)

highest surface roughness-related concerns, as noted in section 5.2.2. Additionally, for inclined up-skin surfaces in diagonal struts, a 'stair step' effect is commonly observed, wherein the edges of individual layers during PBF manufacturing is visible alongside effects of partially fused adhered powder [120, 121]. This is caused primarily due to the stepped approximation of curves in inclined surfaces by layers for PBF, which further adds to dimensional inaccuracies of a manufactured lattice structure. In 2D and 3D comparison of a Voronoi lattice structure manufactured using LPBF shown in Figure 11, numerous dimensional anomalies of the printed lattice structure (compared to original CAD) can be observed, especially for the horizontal and diagonal struts which consist of down-skin surface areas. Additionally, nodes within strut based lattices are known to be regions with highest dimensional inaccuracies and defects [101], especially when compared to surface based lattices [122]. Nodes in strut based lattices are complex surfaces which involve a combination of up-skin, down-skin, and vertical surfaces. This complexity adds to the 'stair step' effect [122] alongside effects of partially fused adhered powder [123]. Additionally, there could a compounded effect of joining multiple struts together in the subsequent layers, wherein due to residual stresses caused by large areas, the struts may not converge to a single point in space as observed in the CAD. These issues of geometric fidelity in AM lattices would be deleterious for bone replacement applications, and hence must be evaluated well before use.

X-ray computer tomography (XCT) of AM lattices is the most common method currently used to evaluate the geometric fidelity of printed lattices by comparison of the XCT scanned model with

the original CAD model [124, 125, 101], as also demonstrated in Figure 11. Other methods include scanning electron microscopy (SEM), optical microscopy, and Vernier calliper based comparisons of the AM lattice with the original CAD dimensions [101].

5.2.4. Advanced considerations for trabecular geometry

This review compared trabecular bone micro-architecture to lattice parameters that can be deployed in additive manufacturing. A simplistic model of trabeculae thickness and spacing was used to relate to the lattice parameters of strut thickness and pore size, respectively. However, trabecular bone has a more complex micro-architecture than traditional strut-based lattices and therefore surface-based lattices should be considered more closely in this application. Furthermore, van Lenthe et al recognized that trabecular bone exhibits both rod and plate-like behavior and suggested that a combined strut- and surface-based lattice configuration may best represent the trabecular bone micro-structure, see Figure 12 [16]; such structures can now be closer to attainable from a manufacturability stand point.

Callens et al. proposed a mathematical model for describing local and global trabecular micro-architecture which suggested that bone does not exhibit mean zero curvature, like those exhibited in TMPS structures [15]. Therefore, a stochastic surface-based lattice may be the best selection for modelling trabecular bone. This has been successfully attempted by Kumar et al. [43] and their work should be considered an emerging opportunity for the design titanium lattice architectures for bone replacement and augmentation. Overall, surface lattices have shown success in replicating the mechanical properties of trabecular bone for titanium and titanium alloys and it is recommended that this avenue be pursued further [91].

6. Conclusions

This review covers the breadth of human bone geometry, mechanical properties of cortical and trabecular bone and the attempts made at replacing these tissues with additively manufactured titanium lattice structures. Human bone, particularly trabecular bone varies significantly with age, sex, disease state, skeletal location and region of the individual bones. Therefore, a site specific and function specific design approach should be considered when designing for human bone replacement, repair and augmentation. Titanium lattice structures generated through additive manufacturing have shown success in replicating cortical bone mechanical properties, promoting osseointegration for improved implant fixation and reduction of stress shielding at the bone-implant interface.

Overall, many studies were able to tune lattice parameters to obtain a Young's modulus and compression stiffness within the range of human cortical bone, with challenges in addressing the porous network architecture concomitantly. Cortical bone is roughly 5-15% porosity and titanium lattices with roughly 50-70% porosity were most successful in achieving comparable stiffness and compressive

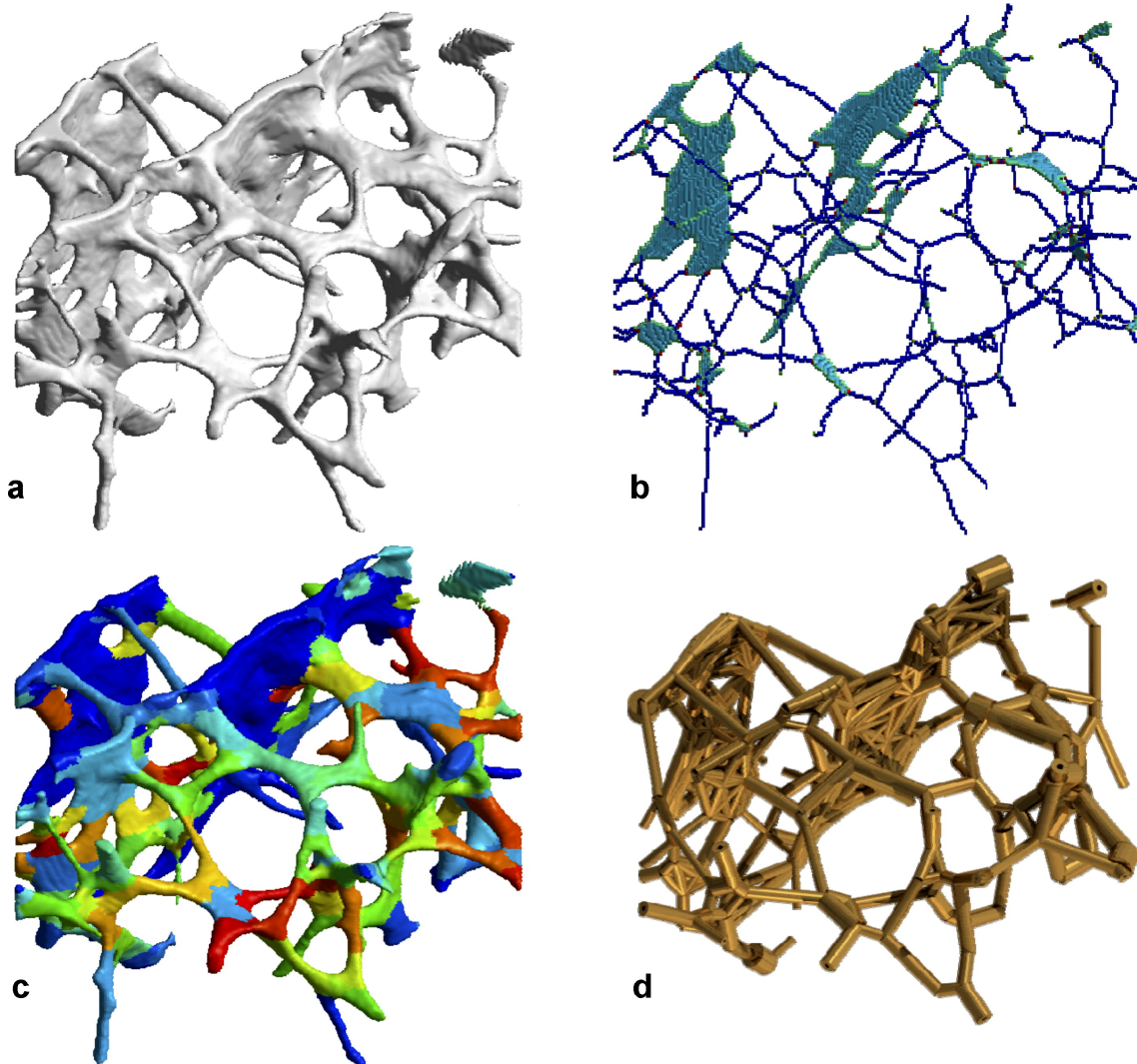


Figure 12: van Length et al., used a micro computed tomographical (micro-CT) image of a human trabecular bone was to develop a specimen-specific beam finite-element model. The process is shown above: (a) micro-CT reconstruction, (b) point cloud generation, (c) multi-colour dilation, and (d) assignment of element thickness and volume to finite element beams. Original figure obtained from [16]

strength. Matching mechanical properties of trabecular bone was less achievable in the current literature. Trabecular thickness, or feature thickness, of human trabecular bone is on the cusp of what is attainable with existing metal additive manufacturing powder bed fusion technologies. Additionally, matching trabecular thickness to feature thickness in titanium-based lattices does not account for the difference in bulk modulus. Therefore, matching feature thickness to trabecular bone thickness is not a recommended technique for matching the mechanical properties of titanium lattice structures to those of human trabecular bone. Control of pore size, porosity and lattice type may yield better results when attempting to replace trabecular bone with additively manufactured titanium lattices.

Future work should include a transfer function that better relates the bulk moduli of titanium and Ti-6Al-4V to the lattice parameters required to generate structures that more seamlessly match the mechanical properties of human cortical and trabecular bone. Due to the large variations in bone porosity and microstructure throughout the human skeleton and the increase of bone porosity with age and in females, patient specific design may yield the best outcome with respect matching mechanical properties of bone with additively manufactured lattices. Improved lattice design for bone replacement and augmentation will allow for improved orthopaedic implant design and may ultimately reduce the risk of stress shielding at the bone implant interface.

7. Acknowledgements

S.P. and M.V. appreciate the funding support received from Federal Economic Development Agency for Southern Ontario (FedDev Ontario grant number 814654). Additionally, S.P. and M.V. would like to acknowledge the help of Jerry Ratthapakdee and Henry Ma with the deployment and characterization of the LPBF builds. M.M. is supported by the Natural Sciences and Engineering Research Council of Canada doctoral scholarship.

References

- [1] Y. Oshida, *Bioscience and bioengineering of titanium materials*, Elsevier, 2010.
- [2] C. Song, A. Wang, Z. Wu, Z. Chen, Y. Yang, D. Wang, The design and manufacturing of a titanium alloy beak for *grus japonensis* using additive manufacturing, *Materials & Design* 117 (2017) 410–416.
- [3] W.-S. Lin, T. L. Starr, B. T. Harris, A. Zandinejad, D. Morton, Additive manufacturing technology (direct metal laser sintering) as a novel approach to fabricate functionally graded titanium implants: preliminary investigation of fabrication parameters., *The International journal of oral & maxillofacial implants* 28 (6) (2013) 1490–1495.

- [4] J. Ong, M. R. Appleford, G. Mani, Introduction to biomaterials: basic theory with engineering applications, Cambridge University Press, 2014.
- [5] C. Emmelmann, P. Sander, J. Kranz, E. Wycisk, Laser additive manufacturing and bionics: redefining lightweight design, *Physics Procedia* 12 (2011) 364–368.
- [6] A. du Plessis, C. Broeckhoven, I. Yadroitsava, I. Yadroitsev, C. H. Hands, R. Kunju, D. Bhate, Beautiful and functional: a review of biomimetic design in additive manufacturing, *Additive Manufacturing* 27 (2019) 408–427.
- [7] L. Murr, K. Amato, S. Li, Y. Tian, X. Cheng, S. Gaytan, E. Martinez, P. Shindo, F. Medina, R. Wicker, Microstructure and mechanical properties of open-cellular biomaterials prototypes for total knee replacement implants fabricated by electron beam melting, *Journal of the mechanical behavior of biomedical materials* 4 (7) (2011) 1396–1411.
- [8] A. Tonino, C. Davidson, P. Klopper, L. Linclau, Protection from stress in bone and its effects. experiments with stainless steel and plastic plates in dogs, *The Journal of bone and joint surgery. British volume* 58 (1) (1976) 107–113.
- [9] X. Tan, Y. Tan, C. Chow, S. Tor, W. Yeong, Metallic powder-bed based 3d printing of cellular scaffolds for orthopaedic implants: A state-of-the-art review on manufacturing, topological design, mechanical properties and biocompatibility, *Materials Science and Engineering: C* 76 (2017) 1328–1343.
- [10] S. Boonen, X. Cheng, J. Nijs, P. Nicholson, G. Verbeke, E. Lesaffre, J. Aerssens, J. Dequeker, Factors associated with cortical and trabecular bone loss as quantified by peripheral computed tomography (pqct) at the ultradistal radius in aging women, *Calcified tissue international* 60 (2) (1997) 164–170.
- [11] J. Spadaro, F. Werner, R. Brenner, M. Fortino, L. Fay, W. Edwards, Cortical and trabecular bone contribute strength to the osteopenic distal radius, *Journal of orthopaedic research* 12 (2) (1994) 211–218.
- [12] X. S. Liu, X. H. Zhang, C. S. Rajapakse, M. J. Wald, J. Magland, K. K. Sekhon, M. F. Adam, P. Sajda, F. W. Wehrli, X. E. Guo, Accuracy of high-resolution in vivo micro magnetic resonance imaging for measurements of microstructural and mechanical properties of human distal tibial bone, *Journal of Bone and Mineral Research* 25 (9) (2010) 2039–2050.
- [13] R. Gauthier, H. Follet, C. Olivier, D. Mitton, F. Peyrin, 3d analysis of the osteonal and interstitial tissue in human radii cortical bone, *Bone* 127 (2019) 526–536.

- [14] S. Majumdar, H. Genant, S. Grampp, D. Newitt, V.-H. Truong, J. Lin, A. Mathur, Correlation of trabecular bone structure with age, bone mineral density, and osteoporotic status: in vivo studies in the distal radius using high resolution magnetic resonance imaging, *Journal of Bone and Mineral Research* 12 (1) (1997) 111–118.
- [15] S. J. Callens, D. C. Tourolle, R. Müller, A. A. Zadpoor, The local and global geometry of trabecular bone, *bioRxiv* (2020).
- [16] G. H. van Lenthe, M. Stauber, R. Müller, Specimen-specific beam models for fast and accurate prediction of human trabecular bone mechanical properties, *Bone* 39 (6) (2006) 1182–1189.
- [17] H. Chen, X. Zhou, H. Fujita, M. Onozuka, K.-Y. Kubo, Age-related changes in trabecular and cortical bone microstructure, *International journal of endocrinology* 2013 (2013).
- [18] B. L. Riggs, L. J. Melton III, R. A. Robb, J. J. Camp, E. J. Atkinson, J. M. Peterson, P. A. Rouleau, C. H. McCollough, M. L. Bouxsein, S. Khosla, Population-based study of age and sex differences in bone volumetric density, size, geometry, and structure at different skeletal sites, *Journal of Bone and Mineral Research* 19 (12) (2004) 1945–1954.
- [19] S. Khosla, B. L. Riggs, E. J. Atkinson, A. L. Oberg, L. J. McDaniel, M. Holets, J. M. Peterson, L. J. Melton III, Effects of sex and age on bone microstructure at the ultradistal radius: a population-based noninvasive in vivo assessment, *Journal of Bone and Mineral Research* 21 (1) (2006) 124–131.
- [20] K. M. Nicks, S. Amin, E. J. Atkinson, B. L. Riggs, L. J. Melton III, S. Khosla, Relationship of age to bone microstructure independent of areal bone mineral density, *Journal of Bone and Mineral Research* 27 (3) (2012) 637–644.
- [21] H. M. Macdonald, K. K. Nishiyama, J. Kang, D. A. Hanley, S. K. Boyd, Age-related patterns of trabecular and cortical bone loss differ between sexes and skeletal sites: a population-based hr-pqct study, *Journal of Bone and Mineral Research* 26 (1) (2011) 50–62.
- [22] J. Aaron, N. Makins, K. Sagreiya, The microanatomy of trabecular bone loss in normal aging men and women., *Clinical orthopaedics and related research* 215 (1987) 260–271.
- [23] E. Seeman, Pathogenesis of bone fragility in women and men, *The Lancet* 359 (9320) (2002) 1841–1850.
- [24] T. Hildebrand, A. Laib, R. Müller, J. Dequeker, P. Rügsegger, Direct three-dimensional morphometric analysis of human cancellous bone: microstructural data from spine, femur, iliac crest, and calcaneus, *Journal of bone and mineral research* 14 (7) (1999) 1167–1174.

- [25] J. S. Thomsen, A. Laib, B. Koller, S. Prohaska, L. Mosekilde, W. Gowin, Stereological measures of trabecular bone structure: comparison of 3d micro computed tomography with 2d histological sections in human proximal tibial bone biopsies, *Journal of Microscopy* 218 (2) (2005) 171–179.
- [26] M. J. Munford, K. G. Ng, J. R. Jeffers, Mapping the multi-directional mechanical properties of bone in the proximal tibia, *Advanced Functional Materials* 30 (46) (2020) 2004323.
- [27] E. F. Morgan, G. U. Unnikrisnan, A. I. Hussein, Bone mechanical properties in healthy and diseased states, *Annual review of biomedical engineering* 20 (2018) 119–143.
- [28] D. L. Bartel, D. T. Davy, *Orthopaedic biomechanics: mechanics and design in musculoskeletal systems*, Prentice Hall, 2006.
- [29] J. Park, R. S. Lakes, *Biomaterials: an introduction*, Springer Science & Business Media, 2007.
- [30] M. A. Velasco, C. A. Narváez-Tovar, D. A. Garzón-Alvarado, Design, materials, and mechanobiology of biodegradable scaffolds for bone tissue engineering, *BioMed research international* 2015 (2015).
- [31] R. W. McCalden, J. A. McGeough, M. B. Barker, et al., Age-related changes in the tensile properties of cortical bone. the relative importance of changes in porosity, mineralization, and microstructure., *The Journal of bone and joint surgery. American volume* 75 (8) (1993) 1193–1205.
- [32] A. H. Burstein, D. T. Reilly, M. Martens, Aging of bone tissue: mechanical properties., *The Journal of bone and joint surgery. American volume* 58 (1) (1976) 82–86.
- [33] S. Peel, D. Eggbeer, Additively manufactured maxillofacial implants and guides—achieving routine use, *Rapid Prototyping Journal* (2016).
- [34] H. E. Burton, S. Peel, D. Eggbeer, Reporting fidelity in the literature for computer aided design and additive manufacture of implants and guides, *Additive Manufacturing* 23 (2018) 362–373.
- [35] W. J. Sames, F. List, S. Pannala, R. R. Dehoff, S. S. Babu, The metallurgy and processing science of metal additive manufacturing, *International materials reviews* 61 (5) (2016) 315–360.
- [36] S. L. Sing, J. An, W. Y. Yeong, F. E. Wiria, Laser and electron-beam powder-bed additive manufacturing of metallic implants: A review on processes, materials and designs, *Journal of Orthopaedic Research* 34 (3) (2016) 369–385.
- [37] Y. M. Wang, T. Voisin, J. T. McKeown, J. Ye, N. P. Calta, Z. Li, Z. Zeng, Y. Zhang, W. Chen, T. T. Roehling, et al., Additively manufactured hierarchical stainless steels with high strength and ductility, *Nature materials* 17 (1) (2018) 63–71.

- [38] A. Casadei, R. Broda, et al., Impact of vehicle weight reduction on fuel economy for various vehicle architectures, Copy obtained from https://www.h3xed.com/blogmedia/Ricardo_FE_MPG_Study.pdf (2007).
- [39] R. Mines, S. Tsopanos, Y. Shen, R. Hasan, S. McKown, Drop weight impact behaviour of sandwich panels with metallic micro lattice cores, *International Journal of Impact Engineering* 60 (2013) 120–132.
- [40] I. Gibson, D. Rosen, B. Stucker, M. Khorasani, *Additive manufacturing technologies*, Vol. 17, Springer, 2014.
- [41] G. Dong, Y. Tang, Y. F. Zhao, A survey of modeling of lattice structures fabricated by additive manufacturing, *Journal of Mechanical Design* 139 (10) (2017).
- [42] G. Maliaris, E. Sarafis, Mechanical behavior of 3d printed stochastic lattice structures, in: *Solid State Phenomena*, Vol. 258, Trans Tech Publ, 2017, pp. 225–228.
- [43] S. Kumar, S. Tan, L. Zheng, D. M. Kochmann, Inverse-designed spinodoid metamaterials, *npj Computational Materials* 6 (1) (2020) 1–10.
- [44] R. J. Mobbs, M. Coughlan, R. Thompson, C. E. Sutterlin, K. Phan, The utility of 3d printing for surgical planning and patient-specific implant design for complex spinal pathologies: case report, *Journal of Neurosurgery: Spine* 26 (4) (2017) 513–518.
- [45] D. Kim, J.-Y. Lim, K.-W. Shim, J. W. Han, S. Yi, D. H. Yoon, K. N. Kim, Y. Ha, G. Y. Ji, D. A. Shin, Sacral reconstruction with a 3d-printed implant after hemisacrectomy in a patient with sacral osteosarcoma: 1-year follow-up result, *Yonsei medical journal* 58 (2) (2017) 453.
- [46] W. J. Choy, R. J. Mobbs, B. Wilcox, S. Phan, K. Phan, C. E. Sutterlin III, Reconstruction of thoracic spine using a personalized 3d-printed vertebral body in adolescent with t9 primary bone tumor, *World Neurosurgery* 105 (2017) 1032–e13.
- [47] N. Xu, F. Wei, X. Liu, L. Jiang, H. Cai, Z. Li, M. Yu, F. Wu, Z. Liu, Reconstruction of the upper cervical spine using a personalized 3d-printed vertebral body in an adolescent with ewing sarcoma, *Spine* 41 (1) (2016) E50–E54.
- [48] N. Taniguchi, S. Fujibayashi, M. Takemoto, K. Sasaki, B. Otsuki, T. Nakamura, T. Matsushita, T. Kokubo, S. Matsuda, Effect of pore size on bone ingrowth into porous titanium implants fabricated by additive manufacturing: An in vivo experiment, *Materials Science and Engineering: C* 59 (2016) 690–701.

- [49] M. de Wild, R. Schumacher, K. Mayer, E. Schkommodau, D. Thoma, M. Bredell, A. Kruse Gujer, K. W. Grätz, F. E. Weber, Bone regeneration by the osteoconductivity of porous titanium implants manufactured by selective laser melting: a histological and micro computed tomography study in the rabbit, *Tissue Engineering Part A* 19 (23-24) (2013) 2645–2654.
- [50] T. Hilton, N. Campbell, K. Hosking, Additive manufacturing in orthopaedics: Clinical implications, *SA Orthopaedic Journal* 16 (2) (2017) 63–67.
- [51] T. Schouman, M. Schmitt, C. Adam, G. Dubois, P. Rouch, Influence of the overall stiffness of a load-bearing porous titanium implant on bone ingrowth in critical-size mandibular bone defects in sheep, *Journal of the mechanical behavior of biomedical materials* 59 (2016) 484–496.
- [52] S. Arabnejad, B. Johnston, M. Tanzer, D. Pasini, Fully porous 3d printed titanium femoral stem to reduce stress-shielding following total hip arthroplasty, *Journal of Orthopaedic Research* 35 (8) (2017) 1774–1783.
- [53] S.-H. Wu, Y. Li, Y.-Q. Zhang, X.-K. Li, C.-F. Yuan, Y.-L. Hao, Z.-Y. Zhang, Z. Guo, Porous titanium-6 aluminum-4 vanadium cage has better osseointegration and less micromotion than a poly-ether-ether-ketone cage in sheep vertebral fusion, *Artificial organs* 37 (12) (2013) E191–E201.
- [54] J. Biemond, G. Hannink, N. Verdonchot, P. Buma, Bone ingrowth potential of electron beam and selective laser melting produced trabecular-like implant surfaces with and without a biomimetic coating, *Journal of Materials Science: Materials in Medicine* 24 (3) (2013) 745–753.
- [55] W. Xue, B. V. Krishna, A. Bandyopadhyay, S. Bose, Processing and biocompatibility evaluation of laser processed porous titanium, *Acta biomaterialia* 3 (6) (2007) 1007–1018.
- [56] J. Van der Stok, O. P. Van der Jagt, S. Amin Yavari, M. F. De Haas, J. H. Waarsing, H. Jahr, E. M. Van Lieshout, P. Patka, J. A. Verhaar, A. A. Zadpoor, et al., Selective laser melting-produced porous titanium scaffolds regenerate bone in critical size cortical bone defects, *Journal of Orthopaedic Research* 31 (5) (2013) 792–799.
- [57] P. K. Srivas, K. Kapat, P. Dadhich, P. Pal, J. Dutta, P. Datta, S. Dhara, Osseointegration assessment of extrusion printed ti6al4v scaffold towards accelerated skeletal defect healing via tissue in-growth, *Bioprinting* 6 (2017) 8–17.
- [58] J. Wieding, T. Lindner, P. Bergschmidt, R. Bader, Biomechanical stability of novel mechanically adapted open-porous titanium scaffolds in metatarsal bone defects of sheep, *Biomaterials* 46 (2015) 35–47.

- [59] S. Van Bael, Y. C. Chai, S. Truscello, M. Moesen, G. Kerckhofs, H. Van Oosterwyck, J.-P. Kruth, J. Schrooten, The effect of pore geometry on the in vitro biological behavior of human periosteum-derived cells seeded on selective laser-melted ti6al4v bone scaffolds, *Acta biomaterialia* 8 (7) (2012) 2824–2834.
- [60] B. Otsuki, M. Takemoto, S. Fujibayashi, M. Neo, T. Kokubo, T. Nakamura, Pore throat size and connectivity determine bone and tissue ingrowth into porous implants: three-dimensional micro-ct based structural analyses of porous bioactive titanium implants, *Biomaterials* 27 (35) (2006) 5892–5900.
- [61] S. Ghouse, N. Reznikov, O. R. Boughton, S. Babu, K. G. Ng, G. Blunn, J. P. Cobb, M. M. Stevens, J. R. Jeffers, The design and in vivo testing of a locally stiffness-matched porous scaffold, *Applied materials today* 15 (2019) 377–388.
- [62] M. Fousová, D. Vojtěch, J. Kubásek, E. Jablonská, J. Fojt, Promising characteristics of gradient porosity ti-6al-4v alloy prepared by slm process, *Journal of the mechanical behavior of biomedical materials* 69 (2017) 368–376.
- [63] S. Arabnejad, R. B. Johnston, J. A. Pura, B. Singh, M. Tanzer, D. Pasini, High-strength porous biomaterials for bone replacement: A strategy to assess the interplay between cell morphology, mechanical properties, bone ingrowth and manufacturing constraints, *Acta biomaterialia* 30 (2016) 345–356.
- [64] K. Moiduddin, S. Darwish, A. Al-Ahmari, S. ElWatidy, A. Mohammad, W. Ameen, Structural and mechanical characterization of custom design cranial implant created using additive manufacturing, *Electronic Journal of Biotechnology* 29 (2017) 22–31.
- [65] O. L. Harrysson, O. Cansizoglu, D. J. Marcellin-Little, D. R. Cormier, H. A. West II, Direct metal fabrication of titanium implants with tailored materials and mechanical properties using electron beam melting technology, *Materials Science and Engineering: C* 28 (3) (2008) 366–373.
- [66] K. Wong, S. Kumta, N. Geel, J. Demol, One-step reconstruction with a 3d-printed, biomechanically evaluated custom implant after complex pelvic tumor resection, *Computer Aided Surgery* 20 (1) (2015) 14–23.
- [67] L. Wang, J. Kang, C. Sun, D. Li, Y. Cao, Z. Jin, Mapping porous microstructures to yield desired mechanical properties for application in 3d printed bone scaffolds and orthopaedic implants, *Materials & Design* 133 (2017) 62–68.

- [68] A. Barbas, A.-S. Bonnet, P. Lipinski, R. Pesci, G. Dubois, Development and mechanical characterization of porous titanium bone substitutes, *Journal of the mechanical behavior of biomedical materials* 9 (2012) 34–44.
- [69] J. Wieding, A. Wolf, R. Bader, Numerical optimization of open-porous bone scaffold structures to match the elastic properties of human cortical bone, *Journal of the mechanical behavior of biomedical materials* 37 (2014) 56–68.
- [70] A. du Plessis, I. Yadroitsava, I. Yadroitsev, Ti6al4v lightweight lattice structures manufactured by laser powder bed fusion for load-bearing applications, *Optics & Laser Technology* 108 (2018) 521–528.
- [71] A. Arjunan, M. Demetriou, A. Baroutaji, C. Wang, Mechanical performance of highly permeable laser melted ti6al4v bone scaffolds, *journal of the mechanical behavior of biomedical materials* 102 (2020) 103517.
- [72] N. Soro, H. Attar, X. Wu, M. S. Dargusch, Investigation of the structure and mechanical properties of additively manufactured ti-6al-4v biomedical scaffolds designed with a schwartz primitive unit-cell, *Materials Science and Engineering: A* 745 (2019) 195–202.
- [73] E. Alabort, D. Barba, R. C. Reed, Design of metallic bone by additive manufacturing, *Scripta Materialia* 164 (2019) 110–114.
- [74] B. Zhang, X. Pei, C. Zhou, Y. Fan, Q. Jiang, A. Ronca, U. D’Amora, Y. Chen, H. Li, Y. Sun, et al., The biomimetic design and 3d printing of customized mechanical properties porous ti6al4v scaffold for load-bearing bone reconstruction, *Materials & Design* 152 (2018) 30–39.
- [75] F. Bartolomeu, M. Costa, N. Alves, G. Miranda, F. Silva, Selective laser melting of ti6al4v sub-millimetric cellular structures: Prediction of dimensional deviations and mechanical performance, *Journal of the Mechanical Behavior of Biomedical Materials* 113 (2021) 104123.
- [76] A. Balcı, F. Küçükaltun, M. F. Aycan, Y. Usta, T. Demir, Reproducibility of replicated trabecular bone structures from ti6al4v extralow interstitials powder by selective laser melting, *Arabian Journal for Science and Engineering* 46 (3) (2021) 2527–2541.
- [77] Y.-Z. Xiong, R.-N. Gao, H. Zhang, L.-L. Dong, J.-T. Li, X. Li, Rationally designed functionally graded porous ti6al4v scaffolds with high strength and toughness built via selective laser melting for load-bearing orthopedic applications, *Journal of the mechanical behavior of biomedical materials* 104 (2020) 103673.

- [78] M. Dallago, S. Raghavendra, V. Luchin, G. Zappini, D. Pasini, M. Benedetti, The role of node fillet, unit-cell size and strut orientation on the fatigue strength of ti-6al-4v lattice materials additively manufactured via laser powder bed fusion, *International Journal of Fatigue* 142 (2021) 105946.
- [79] K. Bari, A. Arjunan, Extra low interstitial titanium based fully porous morphological bone scaffolds manufactured using selective laser melting, *Journal of the mechanical behavior of biomedical materials* 95 (2019) 1–12.
- [80] P. Heintl, L. Müller, C. Körner, R. F. Singer, F. A. Müller, Cellular ti-6al-4v structures with interconnected macro porosity for bone implants fabricated by selective electron beam melting, *Acta biomaterialia* 4 (5) (2008) 1536–1544.
- [81] F. Liu, D. Z. Zhang, P. Zhang, M. Zhao, S. Jafar, Mechanical properties of optimized diamond lattice structure for bone scaffolds fabricated via selective laser melting, *Materials* 11 (3) (2018) 374.
- [82] C. Yan, L. Hao, A. Hussein, P. Young, Ti-6al-4v triply periodic minimal surface structures for bone implants fabricated via selective laser melting, *Journal of the mechanical behavior of biomedical materials* 51 (2015) 61–73.
- [83] M. A. El-Sayed, K. Essa, M. Ghazy, H. Hassanin, Design optimization of additively manufactured titanium lattice structures for biomedical implants, *The International Journal of Advanced Manufacturing Technology* 110 (9) (2020) 2257–2268.
- [84] P. Wang, X. Li, Y. Jiang, M. L. S. Nai, J. Ding, J. Wei, Electron beam melted heterogeneously porous microlattices for metallic bone applications: Design and investigations of boundary and edge effects, *Additive Manufacturing* 36 (2020) 101566.
- [85] X.-Y. Zhang, X.-C. Yan, G. Fang, M. Liu, Biomechanical influence of structural variation strategies on functionally graded scaffolds constructed with triply periodic minimal surface, *Additive Manufacturing* 32 (2020) 101015.
- [86] K. Phan, A. Sgro, M. M. Maharaj, P. D’Urso, R. J. Mobbs, Application of a 3d custom printed patient specific spinal implant for c1/2 arthrodesis, *Journal of Spine Surgery* 2 (4) (2016) 314.
- [87] M. Taheri Andani, C. Haberland, J. M. Walker, M. Karamooz, A. Sadi Turabi, S. Saedi, R. Rahmanian, H. Karaca, D. Dean, M. Kadkhodaei, et al., Achieving biocompatible stiffness in niti through additive manufacturing, *Journal of Intelligent Material Systems and Structures* 27 (19) (2016) 2661–2671.

- [88] J. Ge, J. Huang, Y. Lei, P. O'Reilly, M. Ahmed, C. Zhang, X. Yan, S. Yin, Microstructural features and compressive properties of slm ti6al4v lattice structures, *Surface and Coatings Technology* 403 (2020) 126419.
- [89] D. Zhao, Y. Huang, Y. Ao, C. Han, Q. Wang, Y. Li, J. Liu, Q. Wei, Z. Zhang, Effect of pore geometry on the fatigue properties and cell affinity of porous titanium scaffolds fabricated by selective laser melting, *Journal of the mechanical behavior of biomedical materials* 88 (2018) 478–487.
- [90] E. Marin, M. Pressacco, S. Fusi, A. Lanzutti, S. Turchet, L. Fedrizzi, Characterization of grade 2 commercially pure trabecular titanium structures, *Materials Science and Engineering: C* 33 (5) (2013) 2648–2656.
- [91] I. Yadroitsava, A. du Plessis, I. Yadroitsev, Bone regeneration on implants of titanium alloys produced by laser powder bed fusion: a review, *Titanium for Consumer Applications* (2019) 197–233.
- [92] Y. Zhang, O. Andrukhov, S. Berner, M. Matejka, M. Wieland, X. Rausch-Fan, A. Schedle, Osteogenic properties of hydrophilic and hydrophobic titanium surfaces evaluated with osteoblast-like cells (mg63) in coculture with human umbilical vein endothelial cells (huvec), *dental materials* 26 (11) (2010) 1043–1051.
- [93] L. Liu, P. Kamm, F. García-Moreno, J. Banhart, D. Pasini, Elastic and failure response of imperfect three-dimensional metallic lattices: the role of geometric defects induced by selective laser melting, *Journal of the Mechanics and Physics of Solids* 107 (2017) 160–184.
- [94] A. Charles, A. Elkaseer, L. Thijs, S. G. Scholz, Dimensional errors due to overhanging features in laser powder bed fusion parts made of ti-6al-4v, *Applied Sciences* 10 (7) (2020) 2416.
- [95] C. Druzgalski, A. Ashby, G. Guss, W. King, T. Roehling, M. Matthews, Process optimization of complex geometries using feed forward control for laser powder bed fusion additive manufacturing, *Additive Manufacturing* 34 (2020) 101169.
- [96] X. Wang, K. Chou, Effect of support structures on ti-6al-4v overhang parts fabricated by powder bed fusion electron beam additive manufacturing, *Journal of Materials Processing Technology* 257 (2018) 65–78.
- [97] L. Newton, N. Senin, E. Chatzivagiannis, B. Smith, R. Leach, Feature-based characterisation of ti6al4v electron beam powder bed fusion surfaces fabricated at different surface orientations, *Additive Manufacturing* 35 (2020) 101273.

- [98] K. Cooper, P. Steele, B. Cheng, K. Chou, Contact-free support structures for part overhangs in powder-bed metal additive manufacturing, *Inventions* 3 (1) (2018) 2.
- [99] N. Soro, N. Saintier, J. Merzeau, M. Veidt, M. S. Dargusch, Quasi-static and fatigue properties of graded ti-6al-4v lattices produced by laser powder bed fusion (lpbf), *Additive Manufacturing* 37 (2021) 101653.
- [100] A. Du Plessis, S. M. J. Razavi, F. Berto, The effects of microporosity in struts of gyroid lattice structures produced by laser powder bed fusion, *Materials & Design* 194 (2020) 108899.
- [101] I. Echeta, X. Feng, B. Dutton, R. Leach, S. Piano, Review of defects in lattice structures manufactured by powder bed fusion, *The International Journal of Advanced Manufacturing Technology* 106 (5) (2020) 2649–2668.
- [102] S. Patel, M. Vlasea, Melting modes in laser powder bed fusion, *Materialia* 9 (2020) 100591.
- [103] S. Patel, A. Rogalsky, M. Vlasea, Towards understanding side-skin surface characteristics in laser powder bed fusion, *Journal of Materials Research* 35 (15) (2020) 2055–2064.
- [104] E. Abele, M. Kniepkamp, Analysis and optimisation of vertical surface roughness in micro selective laser melting, *Surface Topography: Metrology and Properties* 3 (3) (2015) 034007.
- [105] Z. Chen, X. Wu, D. Tomus, C. H. Davies, Surface roughness of selective laser melted ti-6al-4v alloy components, *Additive Manufacturing* 21 (2018) 91–103.
- [106] Y. Tian, D. Tomus, P. Rometsch, X. Wu, Influences of processing parameters on surface roughness of hastelloy x produced by selective laser melting, *Additive Manufacturing* 13 (2017) 103–112.
- [107] J. C. Snyder, K. A. Thole, Understanding laser powder bed fusion surface roughness, *Journal of Manufacturing Science and Engineering* 142 (7) (2020).
- [108] Y. Tian, D. Tomus, A. Huang, X. Wu, Experimental and statistical analysis on process parameters and surface roughness relationship for selective laser melting of hastelloy x, *Rapid Prototyping Journal* (2019).
- [109] F. Calignano, Investigation of the accuracy and roughness in the laser powder bed fusion process, *Virtual and Physical Prototyping* 13 (2) (2018) 97–104.
- [110] T. J. Webster, J. U. Ejiófor, Increased osteoblast adhesion on nanophase metals: Ti, ti6al4v, and cocrmo, *Biomaterials* 25 (19) (2004) 4731–4739.

- [111] N. Gui, W. Xu, D. Myers, R. Shukla, H. Tang, M. Qian, The effect of ordered and partially ordered surface topography on bone cell responses: a review, *Biomaterials science* 6 (2) (2018) 250–264.
- [112] S. P. Moylan, J. A. Slotwinski, A. Cooke, K. Jurrens, M. A. Donmez, Lessons learned in establishing the nist metal additive manufacturing laboratory, *NIST technical note* (2013).
- [113] E. Yasa, J. Deckers, T. Craeghs, M. Badrossamay, J.-P. Kruth, Investigation on occurrence of elevated edges in selective laser melting, in: *International Solid Freeform Fabrication Symposium*, Austin, TX, USA, 2009, pp. 673–85.
- [114] L. Chougrani, J.-P. Pernot, P. Véron, S. Abed, Lattice structure lightweight triangulation for additive manufacturing, *Computer-Aided Design* 90 (2017) 95–104.
- [115] G. Shanbhag, M. Vlasea, The effect of reuse cycles on ti-6al-4v powder properties processed by electron beam powder bed fusion, *Manufacturing Letters* 25 (2020) 60–63.
- [116] H. Lee, C. H. J. Lim, M. J. Low, N. Tham, V. M. Murukeshan, Y.-J. Kim, Lasers in additive manufacturing: A review, *International Journal of Precision Engineering and Manufacturing-Green Technology* 4 (3) (2017) 307–322.
- [117] X. Gong, T. Anderson, K. Chou, Review on powder-based electron beam additive manufacturing technology, in: *International Symposium on Flexible Automation*, Vol. 45110, American Society of Mechanical Engineers, 2012, pp. 507–515.
- [118] D. Melancon, Z. Bagheri, R. Johnston, L. Liu, M. Tanzer, D. Pasini, Mechanical characterization of structurally porous biomaterials built via additive manufacturing: experiments, predictive models, and design maps for load-bearing bone replacement implants, *Acta biomaterialia* 63 (2017) 350–368.
- [119] A. Cuadrado, A. Yáñez, O. Martel, S. Deviaene, D. Monopoli, Influence of load orientation and of types of loads on the mechanical properties of porous ti6al4v biomaterials, *Materials & Design* 135 (2017) 309–318.
- [120] G. Strano, L. Hao, R. M. Everson, K. E. Evans, Surface roughness analysis, modelling and prediction in selective laser melting, *Journal of Materials Processing Technology* 213 (4) (2013) 589–597.
- [121] A. Townsend, N. Senin, L. Blunt, R. Leach, J. Taylor, Surface texture metrology for metal additive manufacturing: a review, *Precision Engineering* 46 (2016) 34–47.

- [122] O. Al-Ketan, R. Rowshan, R. K. A. Al-Rub, Topology-mechanical property relationship of 3d printed strut, skeletal, and sheet based periodic metallic cellular materials, *Additive Manufacturing* 19 (2018) 167–183.
- [123] S. Li, H. Hassanin, M. M. Attallah, N. J. Adkins, K. Essa, The development of titanium-based negative poisson's ratio structure using selective laser melting, *Acta Materialia* 105 (2016) 75–83.
- [124] A. Du Plessis, I. Yadroitsev, I. Yadroitsava, S. G. Le Roux, X-ray microcomputed tomography in additive manufacturing: a review of the current technology and applications, *3D Printing and Additive Manufacturing* 5 (3) (2018) 227–247.
- [125] A. M. Vilardell, A. Takezawa, A. Du Plessis, N. Takata, P. Krakhmalev, M. Kobashi, I. Yadroitsava, I. Yadroitsev, Topology optimization and characterization of titanium cellular lattice structures by laser powder bed fusion for biomedical applications, *Materials Science and Engineering: A* 766 (2019) 138330.